Study of the anisotropy in the atomic momentum distributions in a Kapton film

Study of the anisotropy in the atomic momentum distributions in a Kapton film

D Nemirovsky[1], **R Moreh**[1], **Y Finkelstein**[1] **and J Mayers**[2]

[1] Physics Department, Ben-Gurion University of the Negev, Beer-Sheva, Israel
[2] Rutherford Appleton Laboratory, Chilton, Didcot, Oxon OX11 0QX, UK

Abstract
The molecular anisotropy of polymide layers occurring in Kapton
($C_{22}H_{10}N_2O_5$) films was studied using neutron Compton scattering (NCS)
by employing the pulsed neutron source (ISIS) at the Rutherford Appleton
Laboratory (UK). The widths of atomic momentum distributions along and
normal to the Kapton film surface, σ_p and σ_c of the H and C atoms were
obtained together with the corresponding effective temperatures T_p and T_c and
the anisotropy ratio T_p/T_c. The results are interpreted in terms of the in-plane
and out-of-plane zero-point motions of the H and C atoms relative to the film
surface. The data reveal an anisotropy ratio of $T_p/T_c \sim 1.1$ which is far lower
than that deduced when assuming a rigid planar Kapton molecule, where the
ratio is ~ 1.7. The results are in qualitative agreement with calculations based
on the AM1 semi-empirical method included in the GAUSSIAN98 package.

1. Introduction

Kapton (supplied by Dupont) is the commercial name of films made from polymerized
structural units of the form $C_{22}H_{10}N_2O_5$ (figure 1). This molecular structure is usually assumed
to be planar [1, 2], with a small tilt angle between adjacent molecular planes (intra-connected
via –O– bondings). In the polymer itself, all molecules were also thought to be oriented nearly
parallel to the film surface. This assumption was based on the fact that during high temperature
annealing of Kapton films [1, 2] all O and N atoms are released as simple CO, O_2 or N_2 species.
During this process, the hexagons of the molecular unit are left intact and the film contracts
appreciably, resulting in highly-oriented graphite surfaces of a quality comparable to that of
highly-oriented pyrolytic graphite (HOPG) with a mosaic spread of around $2°$.

This behaviour of the graphitized film was attributed to an assumed *planar* well ordered
structure of the initial Kapton polymer film. If true, Kapton may be used as a highly anisotropic
material where the C=C and the C–H bonds are well ordered in the plane, with low energy
vibrations of the atoms normal to the plane. Such a highly anisotropic sample could have been
very useful as a reference calibration line for studies using hydrogen in the EVS spectrometer
and in other applications [3]. It may be noted that Kapton is used as a structural material
and as a window in many experiments involving photon beams. It is also used in a variety of
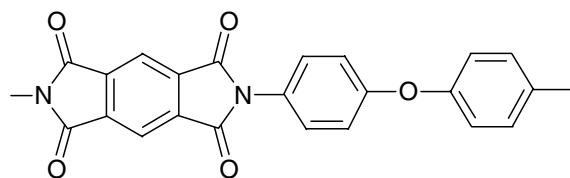
Figure 1. Structural unit in Kapton or pyromellitic dianhydride, PMDA.

electronic insulation applications based on the balance of electrical, thermal, mechanical and chemical properties over a wide temperature range [4].

The purpose of the present work is to test the above expectations by studying the degree of anisotropy in the distribution of atomic momenta of the H and C atoms of the polymide layers at room temperature. This was done by measuring the effective temperatures T_p and T_c of the H and C atoms of Kapton, along and normal to the plane of the film, by using the neutron Compton scattering (NCS) technique. It may be noted that T_p and T_c are related to the corresponding mean square linear momenta $\langle p_p^2 \rangle$ and $\langle p_c^2 \rangle$ of the C atoms by

$$\langle p_c^2 \rangle = MkT_c \qquad \text{and} \qquad \langle p_p^2 \rangle = MkT_p \tag{1}$$

with M the atomic mass and k the Boltzmann constant.

We first discuss the NCS technique and then explain how to calculate effective temperatures of the atoms of the Kapton molecule and also their anisotropy.

1.1. The NCS technique

In the NCS method [5], epithermal neutrons (in the eV energy range) are scattered from single atoms of the sample. The scattered neutrons act as monitors of the directional momentum distributions and kinetic energies (including the part of the zero-point motion) of the scattering atoms. In strongly bound atomic systems such as Kapton, the contribution of the zero-point motion is quite high and any anisotropy is expected to show up as a strong effect even at room temperature.

To obtain the momentum distribution and to interpret the NCS measurements, use is made of the impulse approximation (IA), which is strictly valid only at infinite momentum transfers [6–8]. To do so, consider a neutron transferring momentum $\boldsymbol{Q}$ and energy ε by scattering from an atom of mass m. If the momentum of the atom is $\boldsymbol{p}$ before collision, then momentum conservation requires that it is $\boldsymbol{p} + \boldsymbol{Q}$ after collision, and to conserve kinetic energy, the equation $\varepsilon = [(\boldsymbol{p} + \boldsymbol{Q})^2 - p^2]/2m = (2\boldsymbol{p} \cdot \boldsymbol{Q} + Q^2)/2m$ must be satisfied. Thus the component of atomic momentum along $\boldsymbol{Q}$ is given by:

$$y = \boldsymbol{p} \cdot \boldsymbol{Q}/Q = (2m\varepsilon - Q^2)/2Q. \tag{2}$$

Hence by measuring ε and $\boldsymbol{Q}$ in certain directions, it is possible to deduce $J(Q, y)$ which is the probability that the atomic momentum component along $\boldsymbol{Q}$ is y. Experimentally, our goal was to measure two distributions, $J(Q_p, y)$ and $J(Q_c, y)$ being the distribution of atomic momenta parallel and normal to the Kapton film surface, from which the effective temperatures T_p and T_c were deduced. In our analysis we also accounted for the final state effects (FSE) which were introduced because of the finite momentum transfer $\boldsymbol{Q}$ and the finite energy transfer ε. Such effects were found to increase with the atomic binding and are also inversely proportional to the mass of the scattering atom. The FSE are thus very important in light atoms and are discussed in detail elsewhere [9, 10].

It may be noted that along any intermediate direction making an angle θ with the c-axis, the corresponding effective temperature T_θ is related to T_p and T_c of equation (1) by

$$T_\theta = T_p \sin^2 \theta + T_c \cos^2 \theta. \tag{3}$$

In a *non-oriented* sample, the effective temperature T_e is isotropic and may be expressed in terms of T_p and T_c by
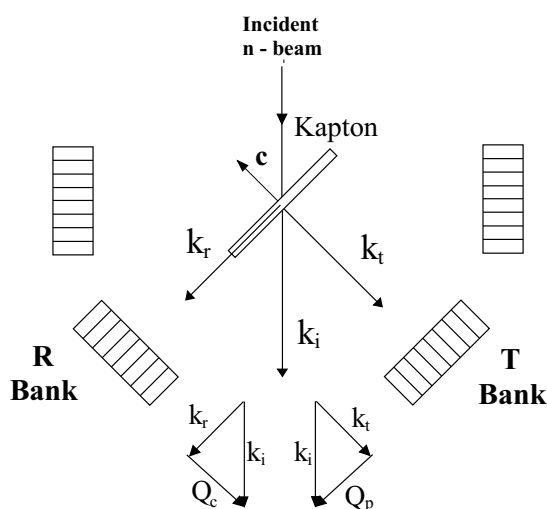
$$T_e = (2T_p + T_c)/3. \tag{4}$$

Figure 2. Schematic diagram of the experimental system showing the incident n-beam, the Kapton sample and two forward banks (each containing eight n-detectors). R and T denote detector banks set along the directions of the *reflected* (R) and *transmitted* (T) neutrons (scattered from H atoms) with respect to the plane of the Kapton sample. k_i is the linear momentum of the incident neutrons; k_t and k_r are those of the scattered neutrons corresponding to momentum transfers Q_p and Q_c along and perpendicular to the plane of the Kapton sample. The relations between the vectors of the scattering process for each of the two geometries are shown in the lower part of the figure for H atoms only.

2. Experimental details

The NCS measurements were carried out using the eVs spectrometer [5] of the ISIS neutron source at the Rutherford Appleton Laboratory (UK). The time of flight (TOF) of the scattered neutrons was measured from the moderator to the detectors, after scattering from the Kapton foil. TOF spectra were taken with and without a resonance absorber of a gold (^{197}Au) foil (placed in front of the detectors), which defined the final neutron energy at 4.912 eV. The shape of the resonance level in ^{197}Au is a Lorentzian having a half width at half maximum of 131 meV, which limits the resolution of the system. The neutrons were detected using 32 Li-glass scintillators arranged in four banks each containing eight detectors (see figure 2). Two banks were positioned around the scattering angles 90° and 270° while the other two were placed at forward angles below 90° and above 270° for the detection of neutrons scattered from hydrogen. With this geometry, it was possible to simultaneously cover the momentum distributions of the C, O, N and H atoms in directions parallel and normal to the Kapton film surface. More details concerning the eVs spectrometer can be found elsewhere [11].

The Kapton sample (produced by Dupont) consisted of a stack of five rectangular foils, each with dimensions 9.0×4.5 cm^2, making a total thickness of 0.75 mm, held on an aluminium frame at $45°$ to the incident n-beam. The frame was wide enough not to be hit by the n-beam. Figure 2 depicts the momenta k_i, k_r and k_t of the incident and scattered neutrons and also the momenta Q_c and Q_p transferred to the scattering nuclei. This is shown for H atoms at scattering angles of $45°$ and $225°$.
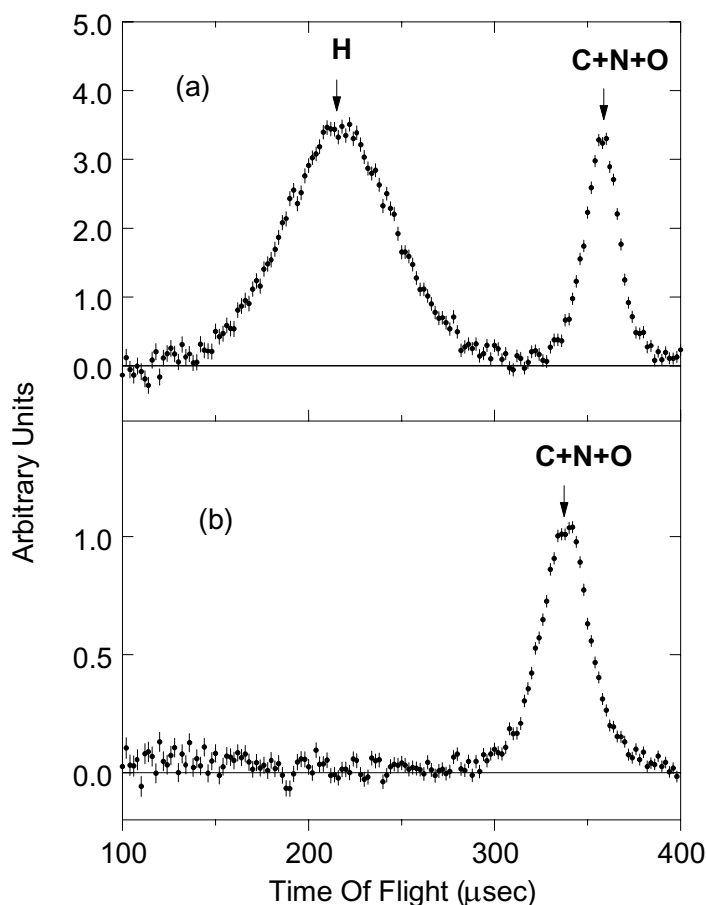

Figure 3. Typical measured TOF spectra of neutrons scattered by the Kapton sample, at scattering angles (a) $55°$ and (b) $100°$. Note that because of kinematics, the H peak appears only at forward scattering angles while disappearing at a scattering angle larger than $90°$.

Figure 3(a) gives the TOF spectrum from a Kapton sample at a scattering angle of $55°$ showing the peak of the H atom together with the combined broad peak of the C, N and O atoms where the corresponding signals are not resolved because of the proximity of the atomic masses and the large width of the instrumental resolution. The TOF spectrum at a large scattering angle, $100°$ (figure 3(b)), reveals only the (C + N + O) peak but no H peak because of the kinematics of n-scattering from hydrogen.

Before extracting the effective temperatures from the TOF spectra, the final state effects were calculated and subtracted [6]. In the case of the H atom, the FSE is large compared to that of the other heavier atoms and is shown in figure 4 as a dashed curve. This gives an idea
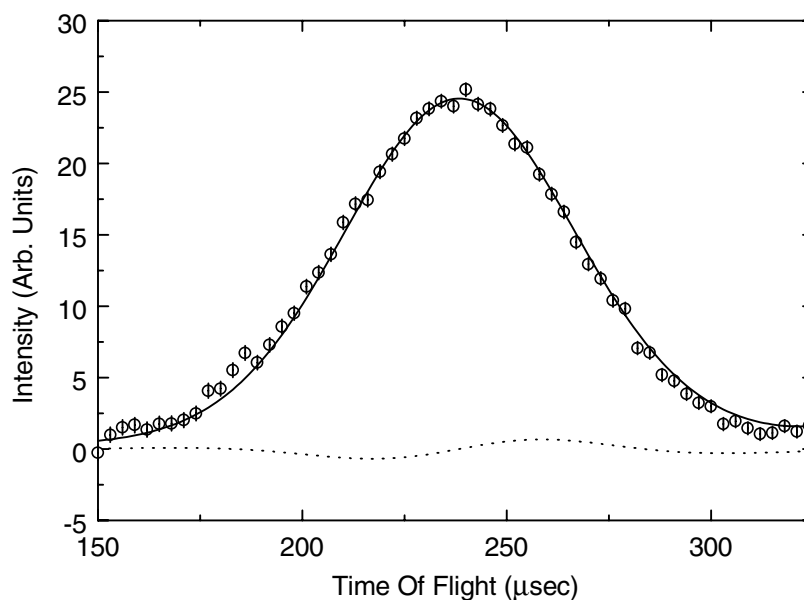
Figure 4. Measured TOF spectrum from a Kapton sample at angle 50.7° showing the H peak and the fitted spectrum after accounting for the FSE. The dashed curve gives the magnitude of the FSE.

about the magnitude of the FSEs for the H atom.

Experimentally, the full width at half maximum (FWHM) widths of each peak in the TOF spectra, which are related to σ_p and σ_c, along and normal to the plane of the Kapton foil, were measured. These are related to the mean square momenta and hence to the effective temperatures T_p and T_c of the scattering atom (such as the H atom), using the relations [12]

$$T_p = h^2\sigma_p^2/4\pi^2 Mk \qquad T_c = h^2\sigma_c^2/4\pi^2 Mk. \tag{5}$$

Equation (5) was used to extract the anisotropy ratio T_p/T_c for the H atom. The same procedure could not be applied to deduce the separate anisotropy ratios for C, N and O atoms, whose contributions could not be resolved. In order to get an idea of the anisotropy for the other three elements, we considered the combined TOF peak of C + N + O and defined an effective mass, which is a weighted average obtained by multiplying the atomic mass of each element by the number of atoms in the molecule and by the scattering cross-section. It may be noted that the value of σ_p/σ_c of the combined peak serves only for getting an idea of the measured anisotropy ratio in the Kapton polymer.

It should be emphasized that the calculated positions of the TOF peaks of C, N and O are separated in time from each other by about 1% at 90° and 270°. Intuitively, one would expect the composite C + N + O peak to be much wider than the pure C peak. It turned out however, the composite peak (contributed dominantly by C) is slightly *narrower* by ∼1.5% than the pure C peak as can be seen from a quantitative simulation of the TOF spectra. This somewhat amazing result is due to the fact that the calculated effective temperatures of the N and O atoms were found to be smaller than that of carbon (see below), causing the actual widths of the pure N and O peaks to be narrower than that of the pure C peak. Thus, the width of the C + N + O peak in the present case is a good measure of the anisotropy in the parallel and perpendicular atomic momenta.

The composite peak was used for deducing the effective temperature of the C atom by taking the values of the N and O atoms from the results of the GAUSSIAN98 AM1 code (see

Table 1. Measured widths σ_p and σ_c of the H atom and the combined (C + N + O) atoms (see figure 3(a)) obtained after applying multiple scattering corrections. The quantity $(\sigma_p/\sigma_c)^2$, related to the ratio of the effective temperatures, is also given. Note the magnitude of the measured anisotropy ratio, which is 1.10. The asterisks refer to the effective temperatures of the C atoms deduced from the combined (C + N + O) peak by taking the σ_p and σ_c values of the N and O atoms from the results of the GAUSSIAN98 AM1 code after assuming an anisotropy ratio of 1.10 for these two atoms.

	Measured	
	H	C + N + O
σ_p (Å^{-1})	4.61 (0.10)	13.21 (0.25)
σ_c (Å^{-1})	4.39 (0.10)	12.64 (0.25)
$(\sigma_p/\sigma_c)^2$	1.10 (0.07)	1.092 (0.06)
	H	C
T_p (K)	1023 (33)	705 (23)*
T_c (K)	927 (33)	644 (20)*
T_p/T_c	1.104 (0.05)	1.095 (0.05)*
T_e (K)	991 (33)	685 (22)*

below) after assuming the same anisotropy ratio for the two atoms, namely 1.10. The results are given in table 1 which shows that the anisotropy ratio T_p/T_c for both the H and C atoms is around 1.10 and is much lower than originally expected.

The performance of the EVS instrument was tested by using a Papyex [12] sample (a commercial form of partially oriented graphite), widely used in adsorption studies. The effective dimensions of the sample and the detector geometry were the same as that of the Kapton measurement. The effective temperatures of the C atoms, in Papyex [12] at 295 K, in directions parallel and normal to the Papyex plane, were determined: $T_p = 815$ K and $T_c = 530$ K and hence highly anisotropic. The data were in good agreement and consistent with the results of a previous study [13] using an HOPG sample. This agreement gave us confidence in the present results and in the reliability of using the NCS technique and the EVS instrument for the present study. It may be noted that any increment of T_p and T_c above 295 K is contributed by the zero-point motion of the C atoms in Papyex and illustrates the suitability of the NCS method for monitoring the anisotropy in the case of Kapton.

In the following, the calculation of T_p and T_c of the H, C, N and O atoms of Kapton, and their relation to the measured quantities is explained.

3. Effective temperatures of the atoms in Kapton

As mentioned in section 1, the effective temperature gives a measure of the total linear momenta, including that of the zero point motion of the scattering atom. For planar molecules, the effective temperature is expected to be highly directional, having a maximum, T_p, along the plane and minimum, T_c, normal to the plane. We hereby illustrate the calculation of the average effective temperatures of the C atoms in a single Kapton molecule ($C_{22}H_{10}N_2O_5$). To do so, we had to terminate the molecule on both ends by an aromatic ring to form a symmetrical structure (figure 5(a)). Thus instead of 39 atoms which the Kapton monomer contains, we get $C_{34}H_{20}N_2O_6$, involving 62 atoms in the calculation.

Note that not all the bonds of the C atoms in Kapton are equivalent: out of 34 C atoms, 20 have C–H bonds and the rest have C=C, C–O, and C–N bonds. Since the molecule has $N = 62$ atoms, it has a total of $3N - 6 = 180$ independent internal normal vibrational modes,
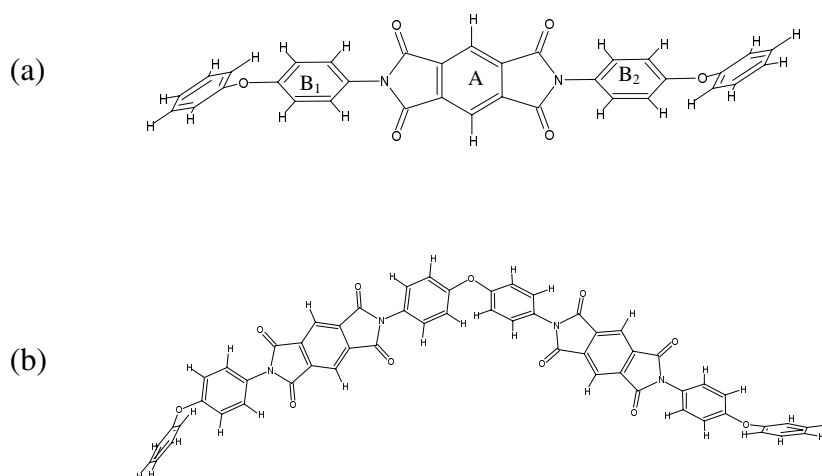
Figure 5. Results of optimization of Kapton molecules obtained using a GAUSSIAN98 AM1 semi-empirical algorithm: (a) for a single molecule; (b) for two molecules.

which should all be accounted for in calculating the effective temperature. The procedure is to consider each mode and find the kinetic energy fraction shared by each of the C atoms in the particular mode. A summation over the contributions from all modes is then carried out. Finally, one has to average out over all C atoms of the molecule. A similar procedure was followed for the H, N and O atoms.

The total kinetic energy of the C atom may be written as $3kT_e/2$. It has contributions from the three kinetic energy components of the *entire* Kapton molecule, consisting of translation ($3kT/2$), libration–rotation ($3kT/2$) and internal vibrations ($\sum_1^{3N-6} k\alpha_j/2$). The factor $1/2$ in this last term arises from the fact that the *kinetic* energy is equal to half the energy of the $3N-6$ vibrational terms, each represented by a harmonic oscillator. The C atom shares only a fraction S_k ($k = t, r, j$) in each kinetic energy term. Thus we may write

$$T_e = (S_t + S_r)T + \frac{1}{3}\sum_{j=1}^{180} S_j\alpha_j \tag{6}$$

where S_t, S_r, S_j ($j = 1, \ldots, 180$) are the energy fractions shared by the C atom in the translational, librational and the jth internal vibrational motions of the entire Kapton molecule; T is the thermodynamic temperature. To be precise, one should also account for the binding effects of translation and libration–rotation of the entire Kapton molecule by using another effective temperature. At 295 K, however, the contribution of this effect is small and was ignored.

The total energy $k\alpha_j$ of each vibrational mode of frequency ν_j, represented as a harmonic oscillator, is

$$k\alpha_j = h\nu_j[(\exp(h\nu_j/kT) - 1)^{-1} + 1/2]. \tag{7}$$

The energy fraction S_t of the C atom is obtained from the translational kinetic energy term of the whole molecule by multiplying by the mass ratio, hence $S_t = M(\text{C})/M(\text{C}_{34}\text{H}_{20}\text{N}_2\text{O}_6) = 12/570$. Similarly, the fraction S_r is deduced from the librational energy of the whole molecule by considering the axes of rotation and the exact geometry of the molecule (figure 5(a)). S_j is obtained by noting that it is equal to the ratio of the vibrational energy of the jth atom relative

to that of the entire molecule:

$$S_j = 4\pi \nu_j^2 M_i A_{ij}^2 / (4\pi \nu_j^2 \sum_{i=1}^{62} M_i A_{ij}^2) \qquad (8)$$

with A_{ij} the amplitude of the ith atom in the jth vibrational mode of the molecule; these are deduced by utilizing computational methods of infrared spectroscopy [14]. To do so, we used the computer code GAUSSIAN98, which yields the normal coordinate values for each atom in each internal vibrational mode of the molecule and along each one of the main molecular axes. S_j is deduced by squaring the calculated normal coordinate and multiplying by the relevant nuclear mass. It was computed separately for each one of the three principal axes of the Kapton film, yielding the effective temperature along any molecular direction. Note that the resulting T_e is the average over that of the 34 C atoms of the Kapton molecule. We now turn to the calculation of S_r. This is obtained by using a summation rule which says that the sum of all energy fractions over all modes of motions (external and internal) is equal to unity, namely $S_t + S_r + \frac{1}{3} \sum_1^{180} S_j = 1$, from which the T_e of the C atom is deduced using equation (5).

To compare the measured data with calculations, it is useful to write the expression of T_e of the C atom along and normal to the surface of an assumed fully oriented Kapton film. Here, we select the plane of the 'skeleton' of one of the Kapton molecules (existing between two N atoms) as coinciding with the plane of the Kapton film. It is thus necessary to define three effective temperatures, along the three principal axes of the molecular film: x, y, z, where the (x, y) plane is that of the Kapton film and z is along the normal to the plane. The effective temperature T_p in the plane of the film is given by

$$T_p = (T_x + T_y)/2. \qquad (9)$$

The calculation of T_i ($i = x, y, z$) is done by projecting each of the 180 normal modes of motion along the above axes, as described in detail elsewhere [15]. A similar calculation was repeated for the H, N, and O atoms. The resulting values of T_p, T_c, their ratio and T_e are listed in table 2. The large difference between these values and the thermodynamic temperature T is purely due to the effect of the zero-point motion and is responsible for the huge anisotropy. A comparison of table 2 and table 1 (for the Kapton molecule depicted in figure 5(a)) shows that the measured anisotropy is much smaller than the calculated value. This means that the overall orientation of molecules of the Kapton film must be quite small and not as revealed in the result for a single molecule. It was thus suspected that by including a larger number of molecules the calculated anisotropy may decrease. To test this point, we repeated the above calculation for two (figure 5(b)), three and four molecules and indeed the ratio T_p/T_c was found to decrease drastically with increasing number of molecules (see table 2).

4. Space orientation of the molecules in Kapton

To understand the reason for the decreasing anisotropy, we studied the space structure of Kapton molecules using an optimization procedure which searched for a minimum in molecular energy. This was done by applying the GAUSSIAN98 package using the AM1 semi-empirical HF model to four separate cases containing one to four Kapton molecules. For clarity, we show in figure 5 the result for the case of a single and two molecules only. Note again that in each case the chain has been terminated in such a way that the molecule formed a symmetrical structure, having an aromatic ring at both ends. The result for a single molecule showed that the planes of the two aromatic rings (B_1 and B_2 in figure 5(a)), situated symmetrically on both sides of the rigid 'skeleton' A (containing the N and O atoms) are parallel to each other and both are tilted at $\sim 30°$ relative to the main molecular plane. The result for two molecules

Table 2. Effective temperatures of the atoms in the one, two, three and four molecules of Kapton as calculated using the GAUSSIAN98–AM1 code. The xy plane is selected to be parallel to one of the rigid 'skeleton' planes. The last column, denoted by an asterisk, lists the corrected values obtained by multiplying all frequencies by a factor of 0.92. The chemical symbols of the molecules used in the calculation are (1) $C_{34}H_{20}N_2O_6$, (2) $C_{56}H_{30}N_4O_{11}$, (3) $C_{78}H_{40}N_6O_{16}$ and (4) $C_{100}H_{50}N_8O_{21}$.

Number of molecules	T_p (K)	T_c (K)	T_p/T_c	T_e (K)	T_e^* (K)
H atom					
1	1406	804	1.75	1205	1114
2	1248	1120	1.11	1205	1114
3	1241	1136	1.09	1206	1115
4	1198	1224	0.98	1206	1115
C atom					
1	866	514	1.68	749	699
2	820	606	1.35	749	699
3	794	662	1.20	750	700
4	761	750	1.04	751	701
N atom					
1	871	364	2.39	702	656
2	862	380	2.27	701	655
3	757	585	1.30	700	654
4	658	720	1.09	700	654
O atom					
1	611	319	1.92	514	487
2	608	380	1.61	532	504
3	527	533	1.01	531	503
4	531	531	1.00	531	503

(figure 5(b)) showed that the distance between the O atoms at each end of the double molecule is 3.22 nm. This is in excellent agreement with a measured value of 3.2 nm, obtained using x-ray diffraction [16]. In addition, a tilt of 8° between the skeleton planes of the two molecules was found to develop. The tilt between two neighbouring hexagons, each belonging to one of the two Kapton molecules and connected via an O atom, is 62°. The unit cell in this polymer seems to consist of two molecules shown in figure 5(b). On increasing the number of molecules included in the calculation to three and then to four, the trend of deviation from coplanarity was found to increase while the ratio of T_p/T_c for the H, C, N, and O atoms was found to approach unity.

It is of interest to note that the calculations using the GAUSSIAN98 code for the case of four molecules of Kapton included 179 atoms and took about 7 days of running time using a PC. Here, one has to consider 537 normal modes and to deduce all the kinetic energy fractions shared by each atom in all modes. Obviously, it was impractical to use *ab initio* calculations because of the huge number of atoms involved.

5. Discussion

It was suspected that the low measured value of the anisotropy ratio T_p/T_c is caused by a smearing effect induced by neutron multiple scattering (MS) and by the high scattering cross-section of the H atoms. This possibility was eliminated by repeating the measurement using thin Kapton of a thickness half that of the above sample, with a smaller anisotropy ratio. The neutron multiple scattering from the H atoms of the sample is expected to increase the effective

temperature by increasing the peak width. The MS corrected values of T_p and T_c are smaller than the measured 'raw' values of the H atom by $\sim$7% while the anisotropy ratio T_p/T_c was increased by $\sim$2%.

This measured anisotropy is consistent with that calculated using the GAUSSIAN98 code, which reveals a small anisotropy when the number of Kapton molecules taken in the calculation becomes three or higher (see table 2). An important consequence of this result is that the relatively small measured anisotropy is very probably created during the manufacturing process of the Kapton, where anisotropic stretching forces and stresses are applied on the film.

From table 2, it is important to note that the measured effective temperatures are lower than the calculated values. This deviation is strongly related to the known problem of frequency scaling in the AM1 semi-empirical method employed in the GAUSSIAN98 code. Such deviations are of the order of 8% for all types of vibration [17]. The extent of deviation varies according to the type of stretching or bending frequency and could be between 4% and as high as 18%. The recommended prescription in the literature is to multiply the calculated frequencies by a factor of $\sim$0.92 to obtain agreement with the measured frequencies. The result of this reduction (see last column of table 2) shows that while a good agreement with experiment is obtained for the case of the C atom, a relatively large deviation ($\sim$12.5%) exists in the H atom.

One point which could affect this deviation is the fact that in our calculations we only considered one chain of molecules and ignored the existence of other neighbouring chains above and below it. The interaction with such chains can in principle reduce further the effective temperature of the atoms and bring T_p and T_c of the H atoms into better agreement with experiment.

Finally, one should note that the above semi-empirical model utilized in GAUSSIAN98 relies on the harmonic approximation. The effect of anharmonicities is expected to be relatively small because these are expected to be large only at low frequencies. However, the effective temperature is defined as the first moment of the frequency spectrum and is determined mainly by the high frequency modes. Hence the contribution of the low frequency modes will be drastically decreased. In addition, since the Kapton polymer was found to be only slightly anisotropic, the contribution of the anharmonicities will be nearly the same for the two directions considered here and hence could be ignored.

Acknowledgments

References

[1] Inagaki M, Harada S, Sato T, Nakajima T, Horino Y and Morita K 1998 *Carbon* **27** 253
[2] Hishiyama Y, Yoshida A, Kaburagi Y and Inagaki M 1992 *Carbon* **30** 333
[3] Kessler E G *et al* 1999 *Phys. Lett.* A **255** 221
[4] Wang P S, Wittberg T N and Wolf J D 1988 *J. Mater. Sci.* **23** 3987
[5] Mayers J, Burke T M and Newport R J 1994 *J. Phys.: Condens. Matter* **16** 641
[6] Sears V F 1984 *Phys. Rev.* B **30** 44
[7] Reiter G and Silver R N 1985 *Phys. Rev. Lett.* **54** 1047
[8] Watson G I 1996 *J. Phys.: Condens. Matter* **8** 5955
[9] Gersch H A and Rodriguez L G 1973 *Phys. Rev.* A **8** 905
[10] Silver R N 1989 *Phys. Rev.* B **39** 4022
[11] Mayers J 1996 *J. Phys.: Condens. Matter* **8** 9423

[12] Finkelstein Y, Nemirovsky D, Moreh R and Kimmel G 2000 *Physica* B **291** 213
[13] Fielding A L, Timms D N and Mayers J 1988 *Europhys. Lett.* **44** 255
[14] Herzberg G 1991 *Infrared and Raman Spectra of Polyatomic Molecules* (New York: Kreiger)
[15] Moreh R, Finkelstein Y and Shechter H 1996 *Phys. Rev.* B **53** 16 006
[16] Kazaryan L G, Tsvankin D Y, Ginzburg B M, Tuycher S, Korzhavin L N and Frenkel S Y 1972 *Visokomol. Soedin.* A **14** 1199
[17] Coolidge M B, Marlin J E and Stewart J J P 1991 *J. Comput. Chem.* **12** 948